Research Square

Preprints are preliminary reports that have not undergone peer review.
They should not be considered conclusive, used to inform clinical practice,
or referenced by the media as validated information.

Superlinear scaling of riverine biogeochemical function with watershed size

Wilfred Wollheim (wil.wollheim@unh.edu)
University of New Hampshire https://orcid.org/0000-0002-5009-3212
Tamara Harms
University of Alaska Fairbanks
Andrew Robison
University of New Hampshire
Lauren Koenig
University of Connecticut https://orcid.org/0000-0002-7790-330X
Ashley Helton
University of Connecticut
Chao Song
Michigan State University https://orcid.org/0000-0001-8225-4490
William Bowden
University of Vermont
Jacques Finlay
University of Minnesota https://orcid.org/0000-0002-7968-7030

Article

Keywords: river networks, carbon and nutrient exchange

Posted Date: January 7th, 2021

DOI: https://doi.org/10.21203/rs.3.rs-137235/v1

License: This work is licensed under a Creative Commons Attribution 4.0 International License.
Read Full License

Version of Record: A version of this preprint was published at Nature Communications on March 9th, 2022. See the published version at https://doi.org/10.1038/s41467-022-28630-z.

Superlinear scaling of riverine biogeochemical function with watershed size

Wilfred M. Wollheim[1*], Tamara K. Harms[2], Andrew L. Robison[1], Lauren E. Koenig[3], Ashley M. Helton[3], Chao Song[4], William B. Bowden[5], Jacques C. Finlay[6]

[1] Department of Natural Resources and the Environment, University of New Hampshire, Durham NH 03824, United States

[2] Department of Biology and Wildlife and Institute of Arctic Biology, University of Alaska Fairbanks, Fairbanks AK 99775, United States

[3] Department of Natural Resources and the Environment, and the Center for Environmental Sciences and Engineering, University of Connecticut, Storrs, CT 06269, United States

[4] Department of Fisheries and Wildlife, Michigan State University, East Lansing, MI 48824, United States

[5] Rubenstein School of Environment and Natural Resources, University of Vermont, Burlington VT 05405, United States

[6] Department of Ecology, Evolution and Behavior, University of Minnesota, St. Paul, MN 55108, United States

* Corresponding author: wil.wollheim@unh.edu, 603-862-5022

Introductory paragraph

River networks are a crucial component of the earth system because they regulate carbon and nutrient exchange between continents, the atmosphere, and oceans. Quantifying the role of river networks at broad spatial scales must accommodate spatial heterogeneity, discharge variability, and upstream-downstream connectivity. Allometric scaling relationships of cumulative biogeochemical function with watershed size integrate these factors, providing an approach for understanding the role of fluvial networks in the earth system. Here we demonstrate that allometric scaling relationships of cumulative river network function are linear (power exponent ~ 1) when biogeochemical reactivity is high and river discharges are low, but become increasingly superlinear (power exponent > 1) as reactivity declines or discharge increases. Superlinear scaling indicates that biogeochemical function of entire river networks within a watershed is an emergent property that increases disproportionately with increasing watershed size. Expanding observation networks will increase precision in riverine fluxes of carbon and nutrients estimated by allometric scaling functions.

Main Text

River networks regulate biogeochemical fluxes from continents to the oceans [1–3] and to the atmosphere [4–9], influencing water quality, coastal dead zones, food webs, and greenhouse gas emissions. For example, at a continental scale, inland waters return ~25% of net carbon uptake by terrestrial ecosystems back to the atmosphere [10]. Similarly, denitrification in river networks removes 20-50% of nitrogen inputs, reducing transfer to oceans while also accounting for a significant proportion of global nitrous oxide emissions [5,11]. Estimating the contribution of river networks to elemental cycles at continental scales remains a challenge due to variation in channel

size and stream flow, which span orders of magnitude [12–14]. Current methodologies prohibit direct measurement of whole-network function and typically encompass little of this variation.

Allometric scaling of cumulative aquatic processes with respect to watershed size offers a synthetic approach that integrates the key attributes of river networks to quantify network-scale biogeochemical function. Allometric scaling described by the metabolic theory of ecology (MTE) has explained variation in metabolism from individual organisms to whole ecosystems [15–17]. Metabolism in individual organisms increases as a power function of body size, with sublinear scaling (log-log slope <1) due to transport constraints through fractal circulatory networks [18]. Sublinear scaling has also been observed for individual lakes and estuaries, where cumulative metabolism increases more slowly than size of the water body due to transport limitation of energy or nutrients [16,17,19]. In contrast, other types of systems, such as cities, exhibit superlinear scaling with increasing size [20].

River network geomorphology is also characterized by fractal networks and exhibits allometric scaling relationships [21,22]. For example, power law scaling describes proportional removal of DOC and total gross primary production, driven by the interaction of biological activity, network structure, and river hydraulics [23–25]. However, it remains unclear why these patterns arise, and how they are influenced by temporal variation in river discharge [13,26]. Here, we demonstrate the range and variability in allometric scaling of river network biogeochemical processes as a function of process rate, river discharge conditions, and network geomorphology (Fig. 1). Using a river network modeling approach (Methods), we quantify the allometric scaling of cumulative biogeochemical function within river networks as they accumulate watershed area between headwaters and the mouths of large river basins. We demonstrate the components that influence scaling relationships and implications for the role of river networks in the earth system.

Superlinear scaling of cumulative river network function with watershed area

Total length and surface area of river channels drives the distribution of material inputs from the watershed and the potential area for biogeochemical processing at river network scales. Scaling of channel length and surface area with watershed size therefore influences cumulative biogeochemical function of the network (Fig. 1). In a diverse subset of observed river networks distributed across different biomes (Supplementary Table 2), cumulative river length scaled nearly linearly with increasing watershed area (mean length slope = 1.06, range 0.99-1.16) (Supplementary Fig. 1A) implying nearly linear scaling of material inputs to river networks, assuming homogenous distribution of runoff and non-point sources. In contrast, cumulative benthic surface area (BSA) in these observed networks scaled superlinearly with watershed area (mean BSA slope = 1.23, range 1.1 – 1.4) (Supplementary Fig. 1B), indicating that surface area of rivers for benthic biogeochemical processes increase faster than watershed size. Theoretical networks of different shapes [24] generated scaling relationships that were similar to the observed networks (See Supplemental Text, Supplementary Fig. 1, Supplementary Table 1, 2). Superlinear scaling of cumulative BSA occurs because as watershed area increases, larger, wider rivers contribute increasingly to cumulative BSA, but relatively less to cumulative length. In the analyses that follow, we use the three different theoretical networks with a range of hydrologic and biological scenarios (Supplementary Table1) to explore scaling of cumulative riverine function with watershed area.

Model scenarios representing variation in river network, biological, and hydrological characteristics (Supplementary Table 1) revealed that allometric scaling relationships between cumulative biogeochemical function and watershed size can range from linear to superlinear. The simplest case, when the local, areal rate for a zero-order process remains constant with

increasing river size (*m.local* = 0, Fig. 1A), results in simple scaling of cumulative riverine function identical to that of BSA as watershed size increases (i.e., superlinearly; cumulative function scaling slope, *d* = 1.23, range of 1.11 to 1.41, Fig. 2). If the local process rate declines with increasing watershed area (*m.local* = -0.5), cumulative function scales nearly linearly (*d* = 1.0, range of 0.95 to 1.09). If *m.local* = 0.5, describing increasing local, areal process rate with increasing watershed area (similar to observations of gross primary productivity [GPP] [27], Supplementary Fig. 2), cumulative processing scales highly superlinearly (mean *d* = 1.64, with range 1.47 to 1.87) (Fig. 2). Thus, the tendency for superlinear scaling of function arising from the scaling of BSA can be offset (approaching linear) or enhanced depending on trends in local process rates with river size as defined by *m.local*. In the case of observed patterns of aquatic GPP [27], superlinearity indicates that aquatic carbon fixation increases disproportionately at the watershed scale as watershed size increases.

To illustrate the importance of superlinear scaling and the utility of this scaling approach, we apply the scaling model with empirical *m.local* for annual mean areal GPP and ecosystem respiration (ER) synthesized for streams with watershed area up to 10,000 km^2 (Supplementary Fig. 2, data from [27]). The resulting scaling function predicts that cumulative riverine CO_2 production (ER – GPP), from a rectangular river network (Supplementary Table 3), increases from a median of 0.23 g m^{-2} yr^{-1} (per unit watershed area) in a first order catchment (A= 1 km^2) to 4.6 g m^{-2} yr^{-1} in a 7th order river network (A = 6321 km^2) (Fig. 3). Similar patterns occur regardless of river network shape or hydraulic assumptions (Supplementary Fig. 3). Although local rates of GPP increase proportionally faster than ER with increasing watershed area (Supplementary Fig. 2, *m.local* for GPP > *m.local* for ER), cumulative riverine CO_2 production increases faster than watershed size because larger rivers continue to be net heterotrophic and

BSA increases at a faster rate than watershed area. The median estimate of CO_2 derived from riverine metabolism for the 7th order watershed (4.6 g m^{-2} of watershed area yr^{-1}) is comparable to a global estimate of 6.7 g m^{-2} yr^{-1}, derived from estimates of total riverine emissions of CO_2 [28] and an average value of riverine contribution to CO_2 flux [9]. We conclude that because of superlinear scaling of BSA and a tendency for increasing GPP and ER (m.local > 0) the contribution of riverine processes to watershed-scale CO_2 emissions increases as watershed area increases, with respiration in large rivers (> 4th order) contributing significantly because of large relative BSA and net CO_2 production.

Discharge influence on allometric scaling in river networks

The analyses above assumed processes were zero-order (i.e., independent of concentration), where material supply from upstream does not affect local areal process rates, and as a result, the magnitude of scaling is independent of flow conditions. In contrast, stream flows determine the magnitude of *d*, the scaling coefficient, for first-order biogeochemical processes (i.e., areal process rate depends on concentration), due to the effect of discharge on downstream source limitation. Scaling of cumulative function for first-order processes shifts from linear under low flows to superlinear under high flows (Fig. 4). As an example, we assume a local, first-order process rate typical of nitrate uptake (uptake velocity, υf = 500 m yr^{-1}, Supplementary Fig. 4), which we assume to be constant with river size [29,30]. When flow and associated material supply from the landscape are low (0.1x mean annual flow), scaling of cumulative processing, *d,* approaches the limit set by the scaling of stream length with watershed size (*d* ~1) (Fig. 5b and Supplementary Fig. 5). That is, material is removed immediately upon entering the river network. At low flows, there is relatively little variability introduced by the

choice of hydraulic geometry (mean d = 0.98, range 0.98 to 1.0, Supplementary Fig. 5). As flows increase, scaling of cumulative function is increasingly superlinear, and at very high flow (20x mean annual flow), d approaches the limit set by BSA scaling (mean d = 1.16, range 1.10 to 1.24 depending on hydraulic scenario, Fig. 4, Supplementary Fig. 5). Similar patterns occur for different network shapes (Supplementary Fig. 5). Synthesis of uptake velocities for different constituents reveals a tendency to increase with discharge, a rough surrogate for watershed area ($m.local$ > 0), though explanatory power is generally weak (r^2 < 0.24, Supplementary Fig. 4 and Table 5). Nevertheless, such an increase would result in an even greater tendency for superlinearity of river network biogeochemical function.

The shift from linear to superlinear scaling with increasing flow can be explained by the changing spatial distribution of riverine uptake relative to biogeochemical inputs from the landscape. Under low flow, material inputs to the river network are low relative to riverine demand, so they are removed near their point of entry and little is transported downstream [13,26]. Material inputs to river networks occur predominantly in headwaters, because of greater total channel lengths and intersection of the landscape [31.] Thus, cumulative processing scales linearly at low flows (d ~ 1), approaching the scaling of channel length (Supplementary Figs. 1A and 5), when materials are primarily processed in the headwaters. In such a scenario, overall removal proportion by the river network is high (Fig. 5A) and processing by larger rivers is limited by low material inputs from upstream.

At high flow, material inputs overwhelm local demand or uptake in headwater streams due to short flowpath length and reduced residence time, resulting in greater downstream material transport and increased opportunity for processing in larger rivers [13]. Scaling of cumulative function then approaches the scaling of BSA (Fig. 5b, Supplementary Fig. 5), with

each unit area of the river network functioning at its maximum areal processing rate as set by the concentration of material inputs from the landscape. Reaction rate determines the range of flows over which superlinear scaling occurs, with lower reaction rates resulting in a broader range flows with superlinear scaling (Fig. 5b, Supplementary Fig. 6), indicating that larger rivers become more important for slower processes across a wider range of flows (e.g., denitrification [3], Supplementary Fig. 4). Note that if scaling of biogeochemical function is in terms of ecosystem size (defined by cumulative river network BSA) rather than watershed size as emphasized here, sublinear scaling occurs under low flow conditions due to transport limitation, similar to that previously reported for individual lakes and estuaries [17] (see Supplemental Text).

Implications of allometric scaling for material fluxes from rivers to atmosphere and ocean

Allometric scaling functions provide useful and succinct estimates of material exchange between river networks and the atmosphere (i.e., cumulative flux of gaseous products) and in regulating material flux to oceans (i.e., proportion of material inputs removed from downstream flux). Our findings show how this role is dependent primarily on flow, reaction rate, and the functional form of the process, as determined by the constituent and the ultimate fate of the product of the process (Fig. 5). Across different carbon and nutrient forms, riverine reaction rates vary over 7 orders of magnitude (Supplementary Fig. 4). Standardized to compare across diverse constituent types (i.e., uptake/piston/settling velocities), reactions rates are highest for gas exchange, nutrient assimilation, particle settling, and respiration of labile DOC, but comparatively low for processing of refractory DOC and denitrification (Supplementary Fig. 4, Supplementary Table 5).

Allometric scaling provides a framework to understand the cumulative uptake, settling, or evasion of varied constituents through watersheds of different sizes. Evasion of terrestrially-derived dissolved gases, including CO_2 (median υ_f ~ 1500 m yr^{-1}, Supplementary Table 5) [32,33], is nearly complete (>90%) across most flow conditions, and occurs primarily in smaller streams because *d* remains nearly linear (Fig. 5). In contrast, river network regulation of downstream nitrate fluxes through permanent removal by denitrification (median υ_f ~ 25 m yr^{-1}, Supplementary Table 5) is more dependent on flow conditions (Fig. 5). At very low flows, network removal proportions are high (~90%), but *d* is superlinear even at relatively low flows, (Fig. 5A, B), indicating that larger rivers play an important role in permanent nitrate removal across all flow conditions. For denitrification, cumulative function increases more slowly with increasing flows (and nitrate supply), indicating that the nitrate removal capacity of the river network becomes saturated (Fig. 5C). Fluxes of nitrous oxide resulting from aquatic denitrification [5,34] will show similar patterns, as would other constituents with relatively low reaction rates, like respiration of refractory DOC. Seasonally varying reaction rates for constituents that are also remobilized (e.g., inorganic N assimilation), will show similar patterns during biologically active times of year, but remobilization at later times will further move materials downstream unless occurring in aquatic ecosystems where retention becomes permanent (such as deeper lakes or reservoirs, not considered here).

The allometric scaling model explains why watershed size is often a poor predictor of nutrient exports from watersheds to oceans [35,36], despite the importance of in-stream processing [37]. Rather than implying that river networks are unimportant in regulating exports from catchments to coasts, a lack of watershed size effect is expected when surface waters are highly reactive, or at low flow. Rapid removal near where constituents enter the river network will

result in no apparent effect of watershed size on export (i.e., d~1; Fig. 5). A watershed size effect should only be apparent in the rare condition of relatively high removal proportion and high scaling exponent, but these combinations tend to occur over only a narrow band of flow conditions for any given reaction rate. Because watershed size effects are usually explored using synoptic surveys that require assumptions of stable, equilibrium flows, or by watershed comparisons at mean annual flows, the watershed size effect is rarely identified empirically, despite high network-scale removal.

Merging observations with scaling theory

The range of scaling exponents identified based on scenarios of river network geomorphology, channel hydraulics, runoff conditions, and biological activity suggests there is no universal scaling law of river network function, in contrast to individual organisms or ecosystems [15,17]. Further, it is likely we have underestimated the range of scaling exponents, given that the simple scaling model presented omits key factors that influence river network biogeochemistry, including biogeochemical activity in the water column of larger rivers [34,38]; hydrologic dynamics in the streambed [39]; ponded waters (including reservoirs and floodplains) [40,41]; saturating reaction kinetics [3]; stoichiometry [42]; climate regime [43]; and spatially heterogeneous material loading [44].

Scaling riverine biogeochemical processes is critical to understanding the role of river networks in the earth system. Under the assumptions of hydraulic geometry and reaction rates presented here, river networks occupying a continental extent contribute disproportionately to global riverine biogeochemical function on a per unit watershed area basis compared to smaller watersheds that drain directly to the coast, particularly at higher flows. Globally, the largest 101

watersheds drain 65% of the earth's land mass [12], yet biogeochemical processes in larger rivers remain understudied compared to small streams [30]. Further, data needed to validate scaling estimates are not available because monitoring networks are typically not designed for nested, network scale analyses within individual watersheds that can be used to further constrain scaling dynamics. River networks therefore remain an important "missing scale" in our observational toolkit of in situ measurements [45]. Superlinear scaling of cumulative biogeochemical processing results from efficient resource use due to disproportionate material inputs from the landscape in headwaters, upstream-downstream connectivity, and high uptake potential downstream, underscoring the role of river networks to functioning of the earth system.

Acknowledgements

This work was supported by the National Science Foundation Macrosystems Biology (MSB-1065255, MSB-1065682, MSB-1442451, MSB-1065055) and Long-Term Ecological Research (PIE-LTER OCE-1637630, ARC-LTER 1637459) programs. Partial support was provided by the New Hampshire Agricultural Experiment Station (NHAES) through USDA National Institute of Food and Agriculture Hatch Project 0225006. This is Scientific Contribution Number 2838.

Author Contributions

WMW, TKH, LEK, AMH, ALR, CS, WBB participated in a workshop where the research was conceptualized. WMW, TKH, AMH, WBB secured funding. JCF contributed the empirical metabolism data and analysis. ALR executed the model scenarios and created Fig. 5. WMW and TKH wrote the paper. All authors contributed to writing and editing,

Methods

Conceptual Overview

For any given biogeochemical process, cumulative aquatic function (F, mass time^{-1}) throughout an entire river network increases with its watershed area (A, km^2). The increase within an individual river network can be defined with a power relationship:

$$F = cA^d \quad (1)$$

where, d is the rate of increase in cumulative aquatic function with watershed area (i.e. allometric scaling) and c is the normalization constant, equivalent to the function in a headwater river network with A = 1 km^2 (Fig. 1).

The scaling of cumulative function (Fig. 1C) accounts for changes in local process rates per unit streambed (benthic) surface area with increasing stream size (Fig. 1A) and accumulation of benthic surface area as watershed area increases (Fig. 1B). Longitudinal variation of a local areal process rate, y (mass benthic area^{-1} time^{-1}), with increasing watershed area of the stream reach (A, km^2) can also be defined with a power function as:

$$y = bA^{m.local} \quad (2)$$

where the constant b represents the local process rate in a stream reach with A = 1 km^2, and $m.local$ is the scaling exponent that describes how the local areal rate changes with increasing stream size as indicated by A (Fig. 1A).

Scaling of cumulative biogeochemical function in stream networks also depends on the scaling of cumulative benthic surface area (Fig. 1B), because biogeochemical activity occurs primarily in the benthos of all but the largest rivers [38,46,47]. The fractal nature of river networks results in cumulative channel length and surface area increasing as a power function of watershed area (Fig. 1B) as influenced by geomorphic attributes of the network (e.g. shape,

number and length of streams in each river order) [23,24]. Scaling of length is due to geomorphic characteristics of the network alone, whereas surface area is also influenced by changes in wetted width as a function of mean discharge that accumulates with watershed area. The relationship between channel width (w) and mean annual discharge (Q) in a downstream direction is described by:

$$w = eQ^f \quad (3)$$

where f typically varies between 0.4 and 0.6 [48,49] and e is the normalization constant. Temporal variation in discharge has a relatively small influence on channel width because the change with discharge at-a-site (in contrast to discharge in the downstream direction) typically has an exponent of only 0.1, until bank full-flood stage is reached [49]. River network structure also determines flow path probabilities [22], which in turn influence biogeochemical function scaling with increasing watershed size.

We quantified the scaling of cumulative biogeochemical function over entire river networks with increasing watershed area using a previously developed statistical river network model [13,26,46]. The model was applied using a range of model parameters constrained by previous studies (Supplementary Table1) to demonstrate the potential envelope of scaling relationships. The model accounts for river network characteristics, including river network geomorphology, the probability of flow paths (upstream-downstream connectivity), flow variability, channel hydraulics, and aquatic biogeochemical processes. We used two types of scenarios to represent biogeochemical processes throughout river networks and to demonstrate scaling for different possibilities of process behavior. The first approach used an areal process rate that is not influenced by local reactant concentration and therefore independent of upstream inputs (i.e., zero-order process rates) but potentially allowed to vary with stream size (Equation 2). The

second approach applied first-order reaction kinetics as is commonly assumed in network models of nutrient or carbon flux [41,47]. In this approach, a reaction rate as uptake velocity ($L\ T^{-1}$) is applied, where the local areal process rate by the stream bottom is then determined by concentration of reactant in the water column. As a result, the local areal uptake within any given stream reach is influenced by the impact of all upstream processes on downstream concentrations. The reaction rate may also vary with stream size (Equation 2). We applied heuristic scenarios of biogeochemical process rates to demonstrate factors controlling scaling relationships, as well as scenarios of actual biogeochemical process rates that explore the implications of the scaling approach for understanding network scale function. To demonstrate the underlying cumulative scaling properties of river networks, the model scenarios also assumed that terrestrial runoff and associated constituent concentrations are spatially uniform.

Physical Structure

River network geomorphology is defined by the number, mean length, and mean watershed areas of streams according to stream order (when two branches of the same order converge, a higher order is created) [22,50]. These characteristics are estimated for each stream order in the model using geomorphological parameters: number ratio R_b; length ratio R_l; area ratio R_a; watershed area and mean length of a first order stream A_1 and L_1, respectively (e.g. Supplementary Table 3). The distributions of where water and non-point material inputs from land initially enter each stream order are estimated from the proportion of watershed area draining 1st order catchments and for higher order streams, the proportion of total stream length in each higher order stream (e.g. Supplementary Table 3). Streams of a given order flow into higher order streams according to probabilities using the Geomorphic Unit Hydrograph approach

[22] which define flow paths through the river network (e.g. Supplementary Table 4). Flow path probabilities are critical in scaling of riverine biogeochemical function because they determine how surface area and biogeochemical processes accumulate with increasing watershed area. They also influence how upstream processes influence the downstream availability of reactants for biogeochemical processes that are concentration dependent.

To explore how scaling potentially varies among different river network geomorphologies, we parameterized the statistical model based on the network attributes of three differently-shaped theoretical channel networks [51]. Theoretical channel networks exhibit the fractal properties observed in natural river networks [22] and were used recently to model river network biogeochemical processes [24,25]. We used them here to demonstrate potential variability in scaling due to network geomorphology. We compared the resulting scaling of length and benthic surface area with increasing watershed area from our statistical model as parameterized from the theoretical networks to the length and benthic scaling in observed river networks derived from digital elevation models of previously studied watersheds [52–54] to ensure consistency (Supplemental Text, Supplementary Fig. 1). We applied geomorphic parameters from all networks to a consistent watershed area of ~6300 km^2 (stream order 6 or 7 at mouth depending on network geomorphic parameters), a watershed area large enough to have a sufficient range of scale to develop the power relationship between cumulative biogeochemical function and watershed area.

In all scenarios, we assumed mean annual runoff over the entire watershed was 500 mm yr^{-1}, a reasonable value for temperate watersheds [55]. Mean annual runoff was used to calculate mean annual discharge (Q m^3 s^{-1}) in each river order using the river order's mean watershed area. Mean discharge was used to estimate the mean width (w), depth (h), and velocity (v) of each

river order using hydraulic geometry equations that describe how *w* changes with mean *Q* in the downstream direction (Equation 3, Supplementary Table1) [48,49]. We explored the role of runoff/discharge variability over time for scenarios with first-order kinetics by varying runoff between 0.1x (roughly baseflow) to 20x (extreme flow) relative to the mean annual runoff. Changes in width, depth, and velocity due to variable discharge at local stream reaches (i.e. "at-a-site") were estimated using at-a-site width vs. discharge equations (*g* in Supplementary Table1). The combination of river network geomorphology, flow path probabilities, runoff, and stream hydraulics determines how reactive surface area scales with increasing watershed area.

Biogeochemical Activity

We used two approaches to represent biogeochemical activity per unit surface area assuming 1) zero-order processes and 2) first-order kinetic processes. An example of a zero-order process is metabolism (gross primary production and ecosystem respiration), which is often represented in streams and rivers as an areal rate (U, M L^{-2} T^{-1}) independent of nutrient concentration [27,56]. An example of a first-order process is nitrogen assimilation or denitrification, which is often represented in streams and rivers as a benthic dominated process using an uptake velocity parameter (υ_f, L T^{-1}), which is equivalent to stream bottom U (M L^{-2} T^{-1}) / water column concentration (C, M L^{-3}) [15]. Both types of activity are considered local rates (Fig. 1B) that may change with stream size (*m.local*) as described in Equation 2. Aquatic processes were aggregated over all streams within each river order as the product of surface area and areal uptake rate. For the first-order kinetics approach, $U = \upsilon_f * C$, where C entering each river order is first predicted by the river network model to account for upstream removal.

River Network Model

For first-order process scenarios, upstream processes influence downstream reactant supply and local areal rates. In the model, the average flux (F, M T^{-1}) exported from rivers of a given river order (which is then routed downstream based on flow path probabilities) is determined as in [26,46]:

$$F = Upstream_{in} * R_{full} + (Local_{in} + Tributary_{in}) * R_{half} \quad \text{Equation 4}$$

$$R_x = 1 - \exp(-\upsilon_f / H_{L\_x}) \quad \text{Equation 5}$$

$$H_{L\_full} = Q_{mid} / (w_{mid} * L) \quad \text{Equation 6}$$

$$H_{L\_half} = Q_{down} / (w_{down} * (L/2)) \quad \text{Equation 7}$$

where $Upstream_{in}$ is the upstream input from the two rivers that initially create the order (M T^{-1}), $Local_{in}$ is the direct input from the landscape as it first enters the river network (M T^{-1}) (Supplementary Table3), $Tributary_{in}$ is the upstream input of additional surface flow paths based on flow path probabilities (e.g. Supplementary Table4, see also [46]) that enter the river along its length (M T^{-1}), R is the removal proportion (unitless), x refers to whether the input travels the entire river length (*full*) or on average half the river length (*half*), H_L is the hydraulic load (L T^{-1}), Q is the mean discharge either at the downstream end (Q_{down}) or the midpoint (Q_{mid}) of the reach length (L^3 T^{-1}), w is mean river width at downstream end or midpoint (L), and L is the mean length of the river order (L). Flow path probabilities are used to identify upstream vs. tributary inputs (e.g. Supplementary Table 4). The model accounts for the removal of constituents by upstream river orders before calculating downstream concentration and uptake. Flow path probabilities are then used to calculate how the biogeochemical process accumulates with increasing watershed size. Linear regression between cumulative quantities against upstream

watershed area on the logarithm scale are used to estimate the regression slope as the scaling exponent for each scenario.

Scenarios

We implemented two sets of model scenarios. The first set explored how the slope of local areal function (*b* in Equation 2) for zero-order process affects the cumulative allometric scaling function (*d* in Equation 1). The second set explored how first order processes interacting with flow conditions affects allometric scaling. We implemented all scenarios with network geomorphology parameters from three different river network shapes derived from optimal channel networks across a range of channel hydraulic parameters (network geomorphology: R_a, R_b, R_l; channel hydraulics: *e*, *f*, *g*; Supplementary Table1). Parameter values are bounded by observed ranges and thus provide the basis for an envelope of potential allometric scaling functions across river network types. Across all scenarios we used constant Watershed Area = 6321 km^2, A_1 = 1 km^2, L_1 = 1 km, and mean annual runoff = 500 mm yr^{-1}.

Allometric scaling for cumulative function vs. watershed area (*d* in Equation 1) takes into account both surface area and biogeochemical activity. For the first set of scenarios, the zero-order kinetic approach for representing biogeochemical activity applied scenarios of local uptake (M L^{-2} T^{-1}) as a function of watershed area (Equation 2, $y = b A^{m.local}$), either increasing (*m.local* > 1), decreasing (*m.local* < 1), or constant (*m.local* = 1, y = b). For an initial heuristic set of scenarios, *m.local* was bounded between -0.5 and 0.5 as a realistic range of possibility to explore how this parameter influences the scaling slope for cumulative function vs. watershed area. For this set of zero-order scenarios, the parameter *b* (local rate for stream sites with watershed area = 1 km^2) was set to an arbitrary level (1 g m^{-2} yr^{-1}), as it does not affect the

scaling relationship for zero-order biogeochemical processes. However, *b* does affect the absolute cumulative function of surface waters.

For the second set of scenarios, first-order kinetics represented local process rates using an uptake velocity (L T^{-1}). The 1st order kinetic scenarios were each run across a range of flow conditions, from 0.1 to 20 times mean annual flow, to explore interactions between biogeochemical demand and flow condition. For simplicity, we assumed loading concentration was constant with variation in flow (i.e. chemostatic). With the assumption of first order reactivity, areal uptake is dependent on concentration ($\upsilon_f = U / C$). Because upstream removal affects downstream concentration, which is also affected by flow conditions [3,26], with first order kinetics the magnitude of υ_f is an important consideration for scaling biogeochemical function with increasing watershed area. To demonstrate scaling, we set υ_f = 500 m yr^{-1} (*b* in Equation 2) representative of nitrate uptake [3,29]. Although there is little empirical evidence that uptake velocities change with river size [3,29,30], in which case *m.local* = 0, some modeling studies do suggest lower values for larger rivers [57,58]. We therefore applied scenarios with *m.local* for uptake velocity = -0.1, 0, and 0.1. We also explored the impact of the uptake velocity constant using scenarios more typical of denitrification (υ_f = 35 m yr^{-1}) [3,59] and ammonium uptake (1000 m yr^{-1}) [29].

Finally, we also applied an empirically-derived zero-order scenario to demonstrate how allometric scaling of biogeochemical function vs. watershed size is relevant to an important issue currently being addressed by the research community, the role of surface waters in the net carbon balance in the earth system [4,9,28]. Functions of local GPP and ER versus watershed area of the river reach (Equation 2) were derived from a broad synthesis of measured stream metabolism [34] across a range of stream sizes (1 - 10,000 km^2). To the GPP and ER data in [27], we fit a linear

regression to the log-log transformed local GPP and ER vs. watershed area in pristine watersheds, resulting in areal GPP (g C m^{-2} of stream bottom yr^{-1}) = 16.4 $A^{0.48}$ and ER (g C m^{-2} of stream bottom yr^{-1}) = 307.1 $A^{0.22}$, where A is watershed area at the stream measurement site in km^2 (Supplementary Fig. 2). Recall that the constant in these equations (*b)* is equivalent to the areal process rate when A = 1 km^2, so b defines processes in small headwater streams. This biological scenario was applied using the river network geomorphology and channel hydraulics in Supplementary Table 1.

References

1. Casas-Ruiz, J. P. *et al.* Delineating the Continuum of Dissolved Organic Matter in Temperate River Networks. *Global Biogeochem. Cycles* **34**, (2020).
2. Galloway, J. N. *et al.* The Nitrogen Cascade. *Bioscience* **53**, 341–356 (2003).
3. Mulholland, P. J. *et al.* Stream denitrification across biomes and its response to anthropogenic nitrate loading. *Nature* **452**, 202–205 (2008).
4. Cole, J. J. *et al.* Plumbing the global carbon cycle: Integrating inland waters into the terrestrial carbon budget. *Ecosystems* **10**, 171–184 (2007).
5. Beaulieu, J. J. *et al.* Nitrous oxide emission from denitrification in stream and river networks. *Proc. Natl. Acad. Sci. U. S. A.* **108**, (2011).
6. Drake, T. W., Raymond, P. A. & Spencer, R. G. M. Terrestrial carbon inputs to inland waters: A current synthesis of estimates and uncertainty. *Limnol. Oceanogr. Lett.* **3**, 132–142 (2018).
7. Butman, D. & Raymond, P. A. Significant efflux of carbon dioxide from streams and rivers in the United States. *Nat. Geosci.* **4**, 839–842 (2011).
8. Yao, Y. *et al.* Increased global nitrous oxide emissions from streams and rivers in the Anthropocene. *Nature Climate Change* vol. 10 138–142 (2020).
9. Hotchkiss, E. R. *et al.* Sources of and processes controlling CO 2 emissions change with the size of streams and rivers. *Nat. Geosci.* **8**, 696–699 (2015).
10. Hayes, D. J. *et al. Chapter 2: The North American carbon budget*. *Second State of the Carbon Cycle Report (SOCCR2): A Sustained Assessment Report* https://carbon2018.globalchange.gov/downloads/SOCCR2_Ch2_North_American_Carbon_Budget.pdf (2018) doi:10.7930/SOCCR2.2018.Ch2.

11. Wollheim, W. M. *et al.* Global N removal by freshwater aquatic systems using a spatially distributed, within-basin approach. *Global Biogeochem. Cycles* **22**, 1–14 (2008).

12. Vörösmarty, C. J., Fekete, B. M., Meybeck, M. & Lammers, R. B. Global system of rivers: Its role in organizing continental land mass and defining land-to-ocean linkages. *Global Biogeochem. Cycles* **14**, 599–621 (2000).

13. Raymond, P. A., Saiers, J. E. & Sobzak, W. V. Hydrological and biogeochemical controls on watershed dissolved organic matter transport: pulse-shunt concept. *Ecology* **97**, 5–16 (2016).

14. Allen, G. H. *et al.* Similarity of stream width distributions across headwater systems. *Nat. Commun.* **9**, 1–7 (2018).

15. Brown, J. H., Gillooly, J. F., Allen, P. A., Savage, V. M. & West, G. B. Toward a Metabolic Theory of Ecology. *Ecology* **85**, 1771–1789 (2004).

16. Glazier, D. Metabolic Scaling in Complex Living Systems. *Systems* **2**, 451–540 (2014).

17. Nidzieko, N. J. Allometric scaling of estuarine ecosystem metabolism. *Proc. Natl. Acad. Sci. U. S. A.* **115**, 6733–6738 (2018).

18. West, G. B., Brown, J. H. & Enquist, B. J. The Fourth Dimension of Life: Fractal Geometry and Allometric Scaling of Organisms. *Science (80-.).* **284**, 1677–1679 (1999).

19. Schramski, J. R., Dell, A. I., Grady, J. M., Sibly, R. M. & Brown, J. H. Metabolic theory predicts whole-ecosystem properties. *Proc. Natl. Acad. Sci. U. S. A.* **112**, 2617–22 (2015).

20. Bettencourt, L. M. A., Lobo, J., Helbing, D., Kühnert, C. & West, G. B. Growth, innovation, scaling, and the pace of life in cities. *Proc. Natl. Acad. Sci. U. S. A.* **104**, 7301–6 (2007).

21. Banavar, J. R., Maritan, A. & Rinaldo, A. Size and form in efficient transportation

networks. *Nature* **399**, 130–132 (1999).

22. Rodriguez-Iturbe, I. & Rinaldo, A. *Fractal river basins: chance and self-organization.* (Cambridge University Press, 1997).

23. Koenig, L. E. *et al.* Emergent productivity regimes of river networks. *Limnol. Oceanogr. Lett.* **4**, 173–181 (2019).

24. Helton, A. M., Hall, R. O. & Bertuzzo, E. How network structure can affect nitrogen removal by streams. *Freshw. Biol.* **63**, 128–140 (2018).

25. Bertuzzo, E., Helton, A. M., Hall, R. O. & Battin, T. J. Scaling of dissolved organic carbon removal in river networks. *Adv. Water Resour.* **110**, 136–146 (2017).

26. Wollheim, W. M. *et al.* River network saturation concept : factors influencing biogeochemical demand of entire river networks relative to supply. *Biogeochemistry* https://doi.org/10.1007/s10533-018-0488-0 (2018).

27. Finlay, J. C. Stream size and human influences on ecosystem production in river networks. *Ecosphere* **2**, art87 (2011).

28. Butman, D. *et al. Chapter 14: Inland Waters. Second State of the Carbon Cycle Report*. https://carbon2018.globalchange.gov/chapter/14/ (2018) doi:10.7930/SOCCR2.2018.Ch14.

29. Ensign, S. H. & Doyle, M. W. Nutrient spiraling in streams and river networks. *J. Geophys. Res.* **111**, G04009 (2006).

30. Tank, J. L., Rosi-Marshall, E. J., Baker, M. A. & Hall, R. O. Are rivers just big streams? A pulse method to quantify nitrogen demand in a large river. *Ecology* **89**, 2935–2945 (2008).

31. Alexander, R. B., Boyer, E. W., Smith, R. A., Schwarz, G. E. & Moore, R. B. The role of

headwater streams in downstream water quality. *J. Am. Water Resour. Assoc.* **43**, 41–59 (2007).

32. Raymond, P. A. *et al.* Scaling the gas transfer velocity and hydraulic geometry in streams and small rivers. *Limnol. Oceanogr. Fluids Environ.* **2**, 41–1597669 (2012).

33. Ulseth, A. J. *et al.* Distinct air–water gas exchange regimes in low- and high-energy streams. *Nat. Geosci.* **12**, 259–263 (2019).

34. Marzadri, A., Dee, M. M., Tonina, D., Bellin, A. & Tank, J. L. Role of surface and subsurface processes in scaling N2O emissions along riverine networks. *Proc. Natl. Acad. Sci. U. S. A.* **114**, 4330–4335 (2017).

35. Alvarez-Cobelas, M., Angeler, D. G. & Sánchez-Carrillo, S. Export of nitrogen from catchments: A worldwide analysis. *Environ. Pollut.* **156**, 261–269 (2008).

36. Caraco, N. F., Cole, J. J., Likens, G. E., Lovett, G. M. & Weathers, K. C. Variation in NO3 export from flowing waters of vastly different sizes: Does one model fit all? *Ecosystems* **6**, 344–352 (2003).

37. Bernhardt, E. S. *et al.* Can't See the Forest for the Stream? The capacity of instream processing to modify terrestrial nitrogen exports. *Bioscience* **52**, 219–230 (2005).

38. Gardner, J. R. & Doyle, M. W. Sediment–Water Surface Area Along Rivers: Water Column Versus Benthic. *Ecosystems* 1–16 (2018) doi:10.1007/s10021-018-0236-2.

39. Gomez-Velez, J. D., Harvey, J. W., Cardenas, M. B. & Kiel, B. Denitrification in the Mississippi River network controlled by flow through river bedforms. *Nat. Geosci.* **8**, 941–945 (2015).

40. Gardner, J. R., Pavelsky, T. M. & Doyle, M. W. The Abundance, Size, and Spacing of Lakes and Reservoirs Connected to River Networks. *Geophys. Res. Lett.* **46**, 2592–2601

(2019).

41. Schmadel, N. M. *et al.* Small Ponds in Headwater Catchments Are a Dominant Influence on Regional Nutrient and Sediment Budgets. *Geophys. Res. Lett.* **46**, 9669–9677 (2019).

42. Taylor, P. G. & Townsend, A. R. Stoichiometric control of organic carbon–nitrate relationships from soils to the sea. *Nature* **464**, 1178–1181 (2010).

43. Doyle, M. W. Incorporating hydrologic variability into nutrient spiraling. *J. Geophys. Res.* **110**, GO1003 (2005).

44. Mineau, M. M., Wollheim, W. M. & Stewart, R. J. An index to characterize the spatial distribution of land use within watersheds and implications for river network nutrient removal and export. *Geophys. Res. Lett.* **42**, **doi:10**, (2015).

45. Ward, A. S. *et al.* Spatial and temporal variation in river corridor exchange across a 5th-order mountain stream network. *Hydrol. Earth Syst. Sci.* **23**, 5199–5225 (2019).

46. Wollheim, W. M., Vörösmarty, C. J., Peterson, B. J., Seitzinger, S. P. & Hopkinson, C. S. Relationship between river size and nutrient removal. *Geophys. Res. Lett.* **33**, 2–5 (2006).

47. Alexander, R. B. B. *et al.* Dynamic modeling of nitrogen losses in river networks unravels the coupled effects of hydrological and biogeochemical processes. *Biogeochemistry* **93**, 91–116 (2009).

48. Leopold, L. B., Wolman, M. G. & Miller, J. P. *Fluvial processes in geomorphology*. (W.H. Freeman and Company, 1964).

49. Knighton, D. Fluvial forms and processes: a new perspective. (1998).

50. Dingman, S. L. *Physical Hydrology*. (Prentice Hall, 1994).

51. Rinaldo, A. *et al.* Minimum energy and fractal structures of drainage networks. *Water Resour. Res.* **28**, 2183–2195 (1992).

52. Rüegg, J. *et al.* Baseflow physical characteristics differ at multiple spatial scales in stream networks across diverse biomes. *Landsc. Ecol.* **31**, 119–136 (2016).

53. Samal, N. *et al.* Projections of Coupled Terrestrial and Aquatic Ecosystem Change Relevant to Ecosystem Service Valuation at Regional Scales. *Ecol. Soc.* **22**, 18. https://doi.org/10.5751/ES-09662–220418 (2017).

54. Wollheim, W. M., Peterson, B. J., Thomas, S. M., Hopkinson, C. H. & Vörösmarty, C. J. Dynamics of N removal over annual time periods in a suburban river network. *J. Geophys. Res.* **113**, G03038 (2008).

55. Fekete, B. M., Vorosmarty, C. J. & Grabs, W. High-resolution fields of global runoff combining observed river discharge and simulated water balances. *Global Biogeochem. Cycles* **16**, 1–10 (2002).

56. Hoellein, T. J., Bruesewitz, D. A. & Richardson, D. C. Revisiting Odum (1956): A synthesis of aquatic ecosystem metabolism. *Limnol. Oceanogr.* **58**, 2089–2100 (2013).

57. Moore, R. B., Johnston, C. M., Smith, R. A. & Milstead, B. Source and delivery of nutrients to receiving waters in the northeastern and mid-atlantic regions of the United States. *J. Am. Water Resour. Assoc.* **47**, 965–990 (2011).

58. Alexander, R. B., Smith, R. A. & Schwarz, G. E. Effect of stream channel size on the delivery of nitrogen to the Gulf of Mexico. *Nature* **403**, 758–761 (2000).

59. Howarth, R. W. *et al.* Regional nitrogen budgets and riverine inputs of N and P for the drainages to the North Atlantic Ocean: natural and human influences. *Biogeochemistry* **35**, (1996).

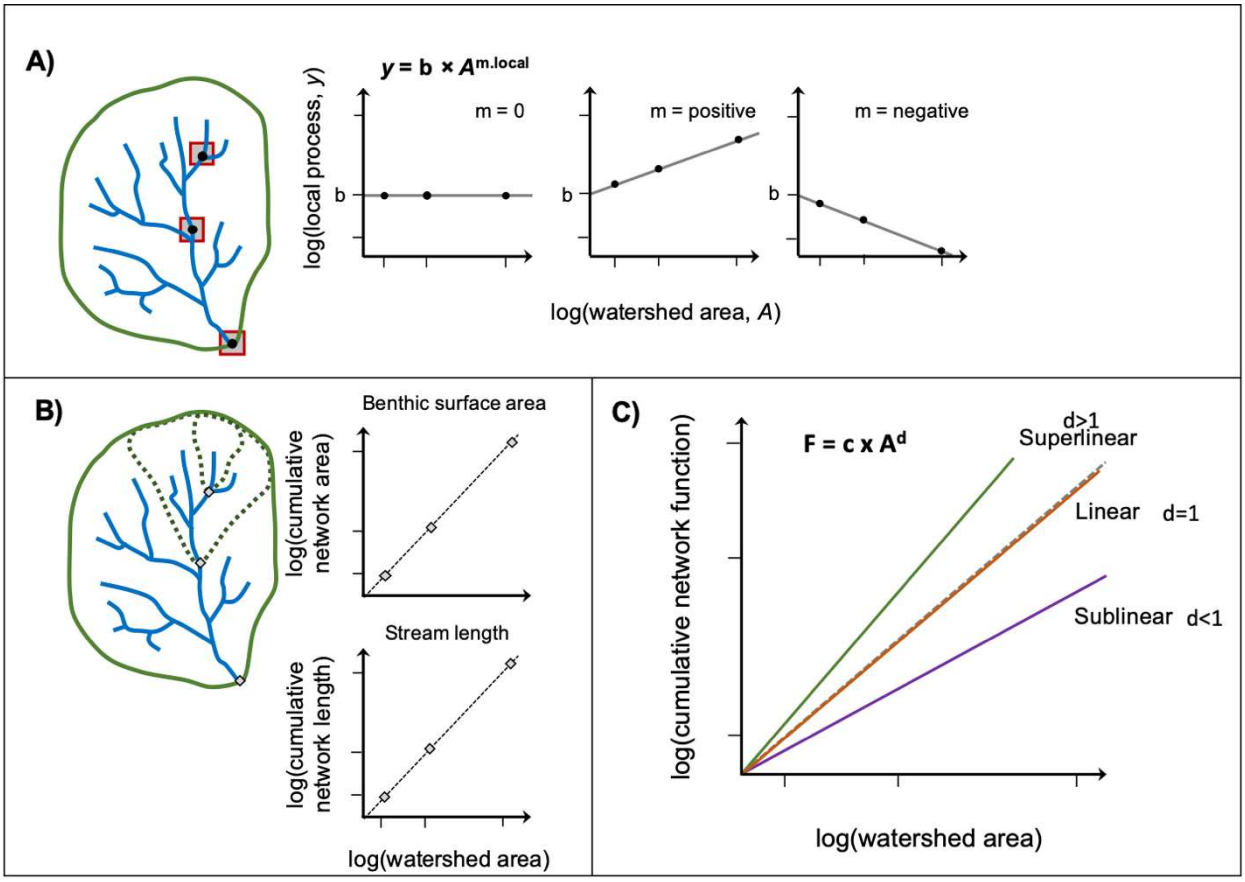

Fig. 1. Conceptual model describing allometric scaling of cumulative biogeochemical function in river networks with watershed area as determined by local areal process rates and river network physical structure. A) Scenarios of the change in local process rate (as either mass benthic area^{-1} time^{-1} or length time^{-1}) in stream reaches (slope = *m.local*, Equation 2) vs. increasing watershed area draining to the stream location. B) Scaling of cumulative benthic surface area and stream length vs. increasing watershed area, accounting for the entire upstream river network. C) Examples of scaling of cumulative biogeochemical function (slope = *d*, Equation 1) with increasing watershed area (mass time^{-1}), resulting from variation in both local process rates (A) and cumulative physical attributes of networks (B).

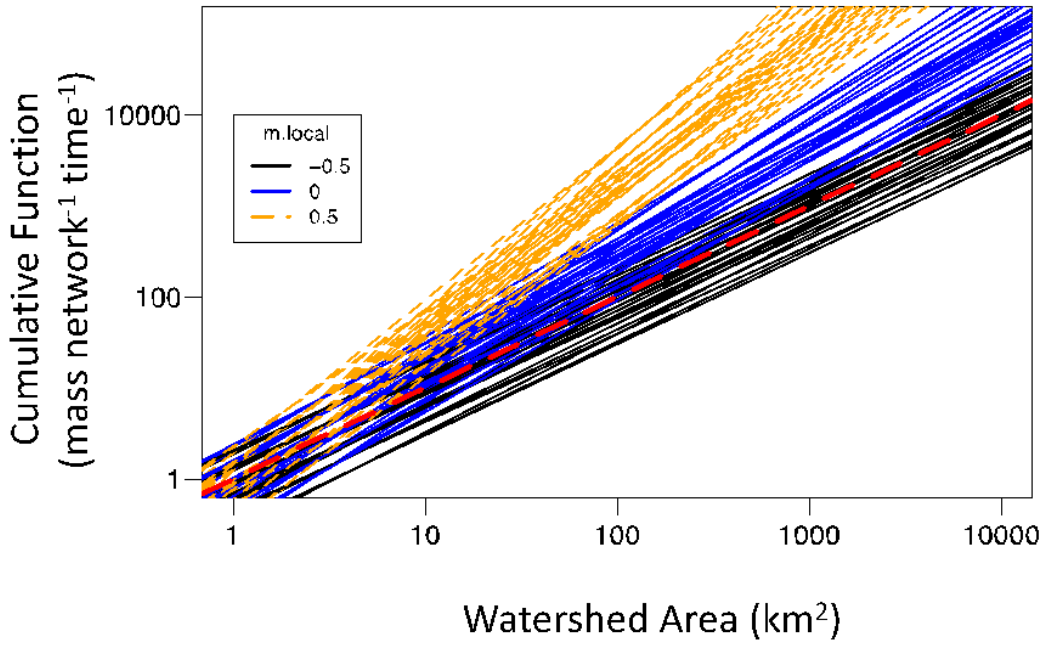

Fig. 2. Cumulative biogeochemical function for zero-order processes, wherein surface water concentrations do not influence local areal process rates. Colors represent scaling of local areal process rate with increasing river size ($y = bA^{m.local}$), where *m.local* = -0.5 (black), 0 (blue), or 0.5 (orange dash). Each line represents a different scenario combining network geomorphology and channel hydraulics (Supplementary Table1). Red dashed line indicates linear scaling.

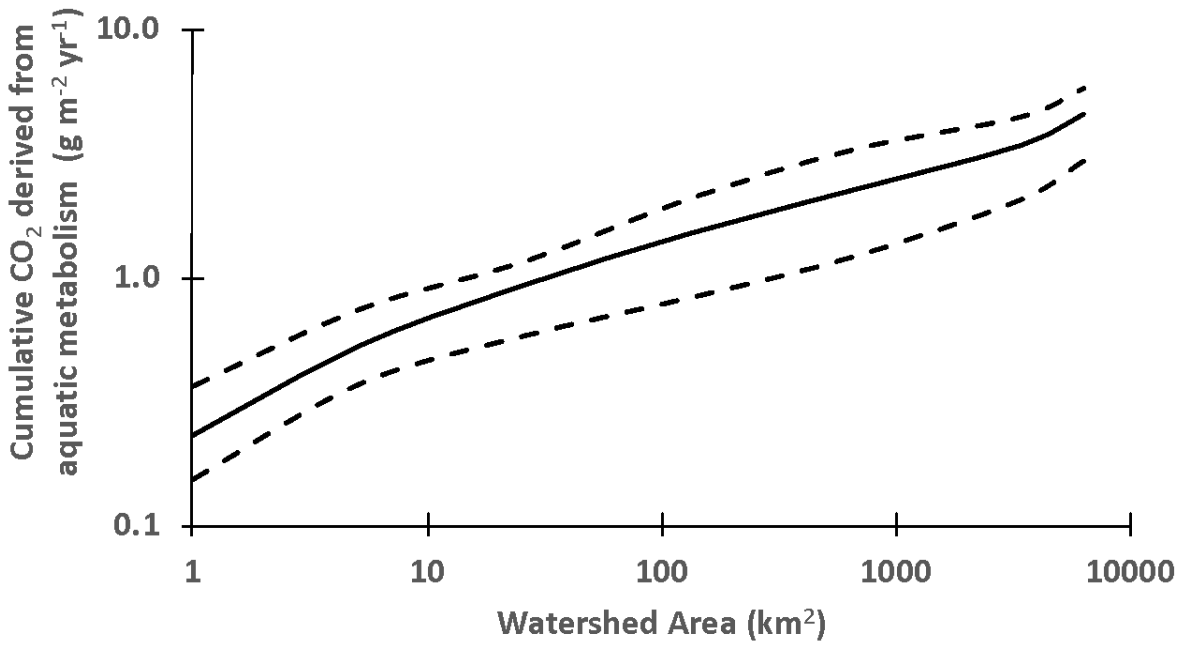

Fig. 3. Cumulative CO_2 derived from aquatic metabolism (cumulative ER - cumulative GPP, normalized to per unit watershed area). Model results incorporate observed trends in the local rate of GPP and ER with watershed area (Supplementary Fig. 2) for a rectangular river network at mean annual flow (500 mm yr^{-1}). Median (solid line), 25th percentile and 75th percentiles (dashed lines) are derived from 9 model scenarios that reflect potential variation in hydraulic dimensions (varying *e* and *f* in Supplementary Table1).

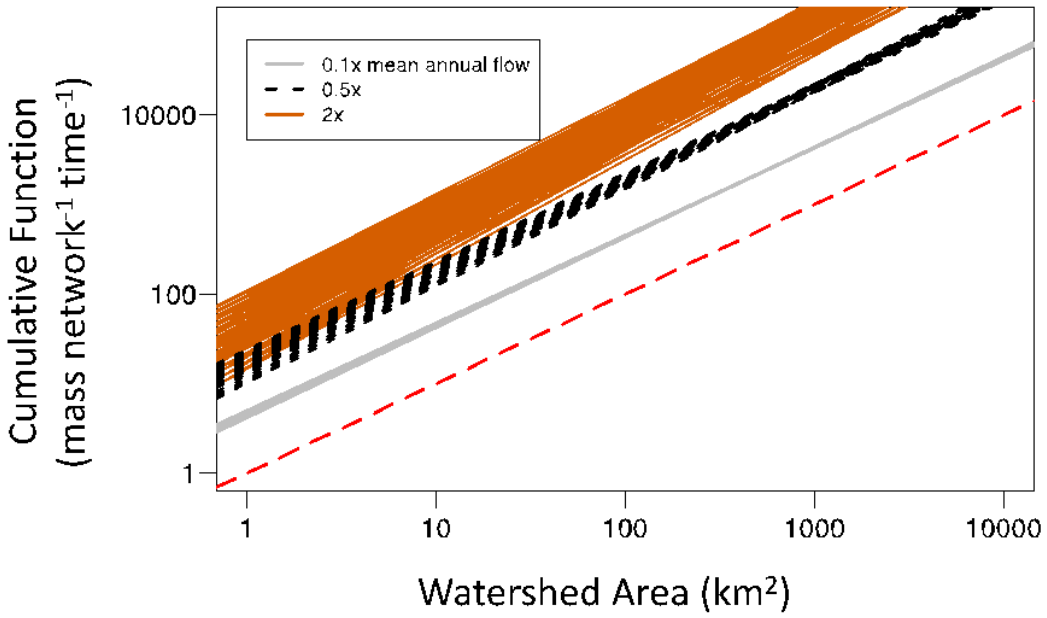

Fig. 4. Cumulative biogeochemical function of first-order processes vs. watershed area at different flows. Colors represent flow conditions as a proportion of mean annual flow: 0.1x mean annual flow (grey), 0.5x (black dashed), and 2x (orange). Red dashed line indicates linear scaling. Model results reflect a rectangular river network with average process rate in a 1 km^2 headwater watershed = 500 m yr^{-1} (*b* in Equation 2). Lines depict potential variation in channel hydraulics and first-order biogeochemical scenarios in Supplementary Table1 (each flow level contains n = 87 scenarios, varying *e*, *f*, *g*, and *m.local* for first order) .

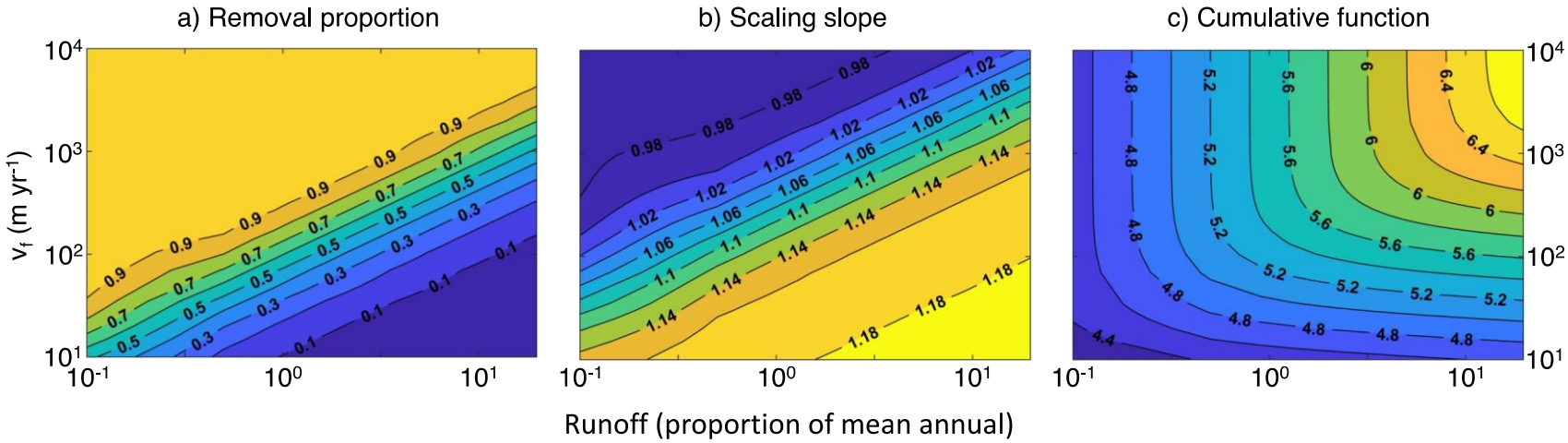

Fig. 5. Model scenarios showing the impact of uptake velocity and runoff (as a proportion of mean annual runoff) on A) mean network scale removal (proportion of inputs from land removed by the entire river network), B) mean scaling slope, *d*, and C) cumulative aquatic function (kg yr^{-1} in the modeled river network). Each v_f and runoff combination is based on the mean of 27 hydraulic scenarios for a rectangular network as described in Supplementary Table1. Contour intervals indicate the value for each isobar boundary.

Figures

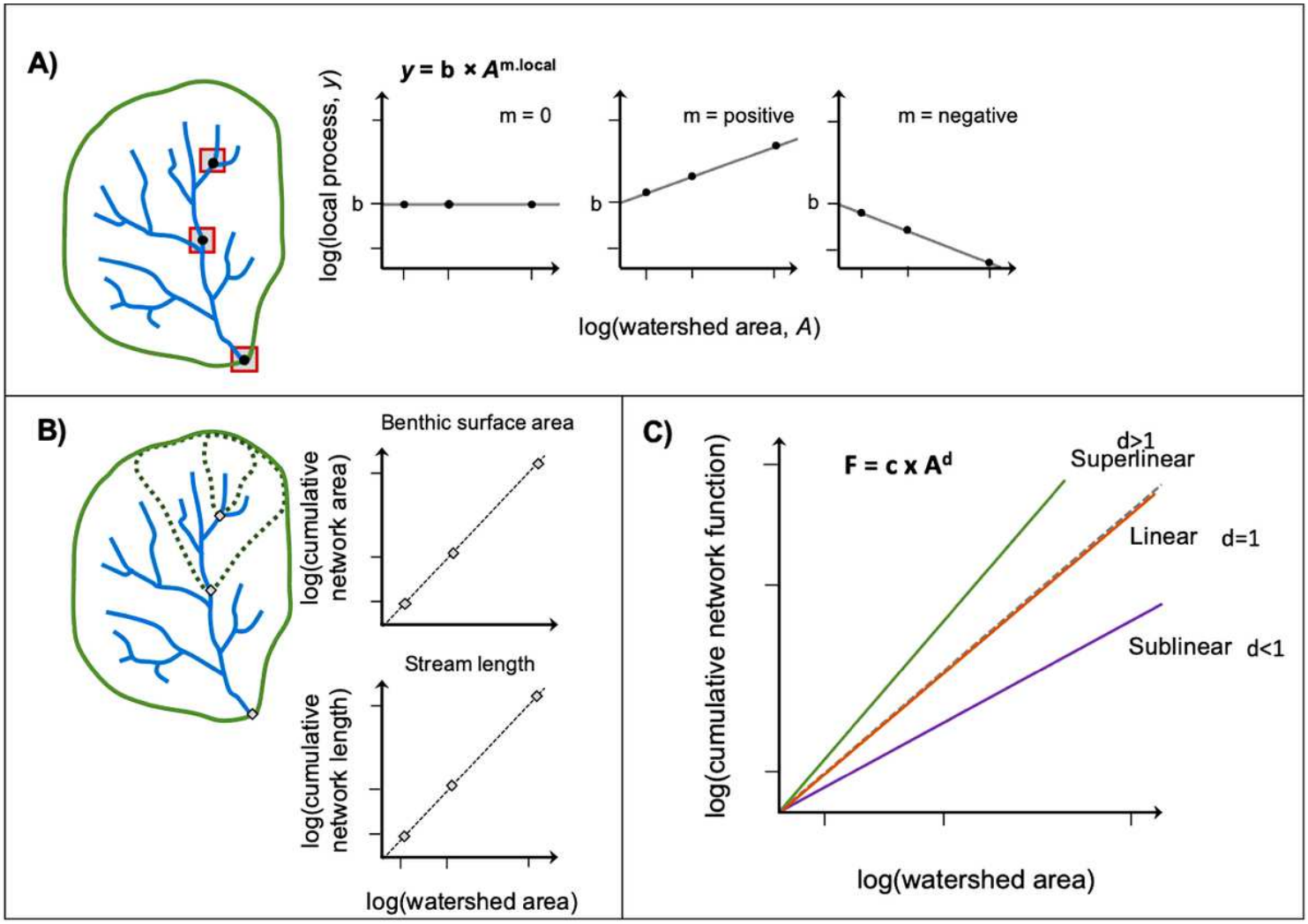

Figure 1

Conceptual model describing allometric scaling of cumulative biogeochemical function in river networks with watershed area as determined by local areal process rates and river network physical structure. A) Scenarios of the change in local process rate (as either mass benthic area-1 time-1 or length time-1) in stream reaches (slope = m.local, Equation 2) vs. increasing watershed area draining to the stream location. B) Scaling of cumulative benthic surface area and stream length vs. increasing watershed area, accounting for the entire upstream river network. C) Examples of scaling of cumulative biogeochemical function (slope = d, Equation 1) with increasing watershed area (mass time-1), resulting from variation in both local process rates (A) and cumulative physical attributes of networks (B).

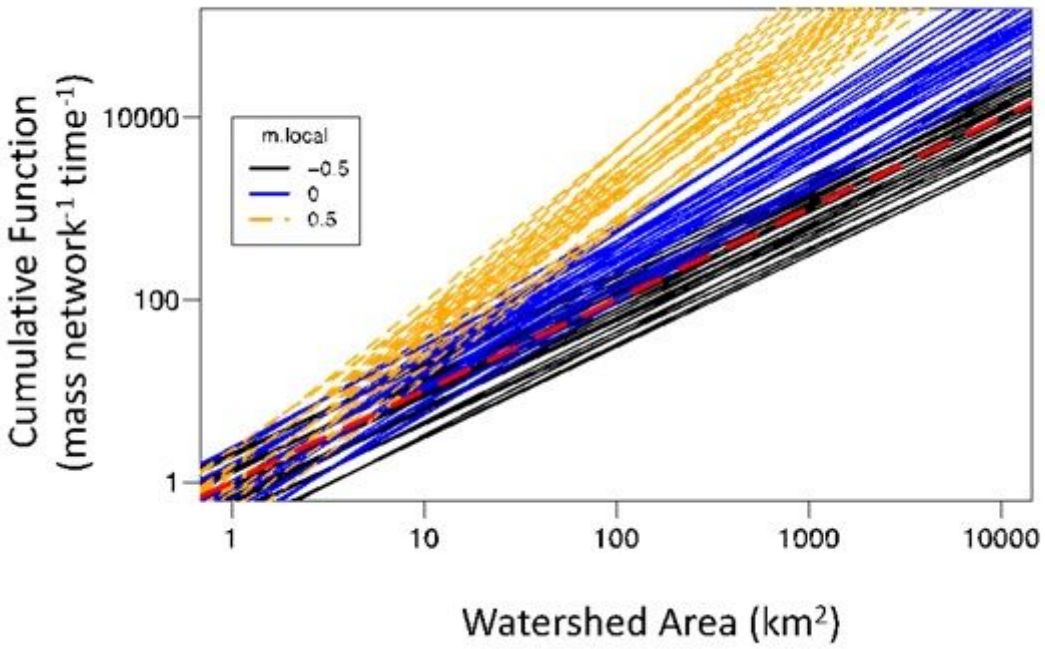

Figure 2

Cumulative biogeochemical function for zero-order processes, wherein surface water concentrations do not influence local areal process rates. Colors represent scaling of local areal process rate with increasing river size (y = bAm.local), where m.local = -0.5 (black), 0 (blue), or 0.5 (orange dash). Each line represents a different scenario combining network geomorphology and channel hydraulics (Supplementary Table1). Red dashed line indicates linear scaling.

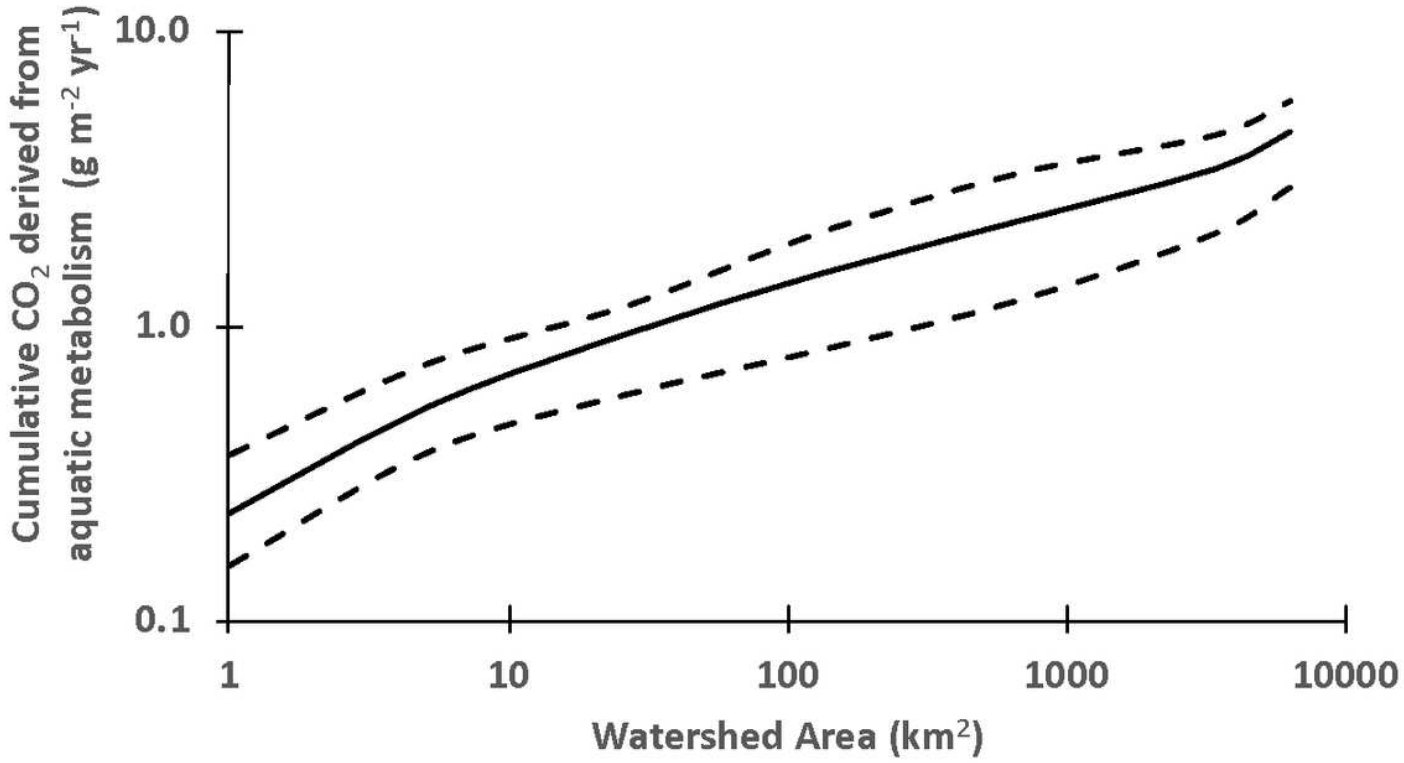

Figure 3

Cumulative CO2 derived from aquatic metabolism (cumulative ER - cumulative GPP, normalized to per unit watershed area). Model results incorporate observed trends in the local rate of GPP and ER with watershed area (Supplementary Fig. 2) for a rectangular river network at mean annual flow (500 mm yr-1). Median (solid line), 25th percentile and 75th percentiles (dashed lines) are derived from 9 model scenarios that reflect potential variation in hydraulic dimensions (varying e and f in Supplementary Table1).

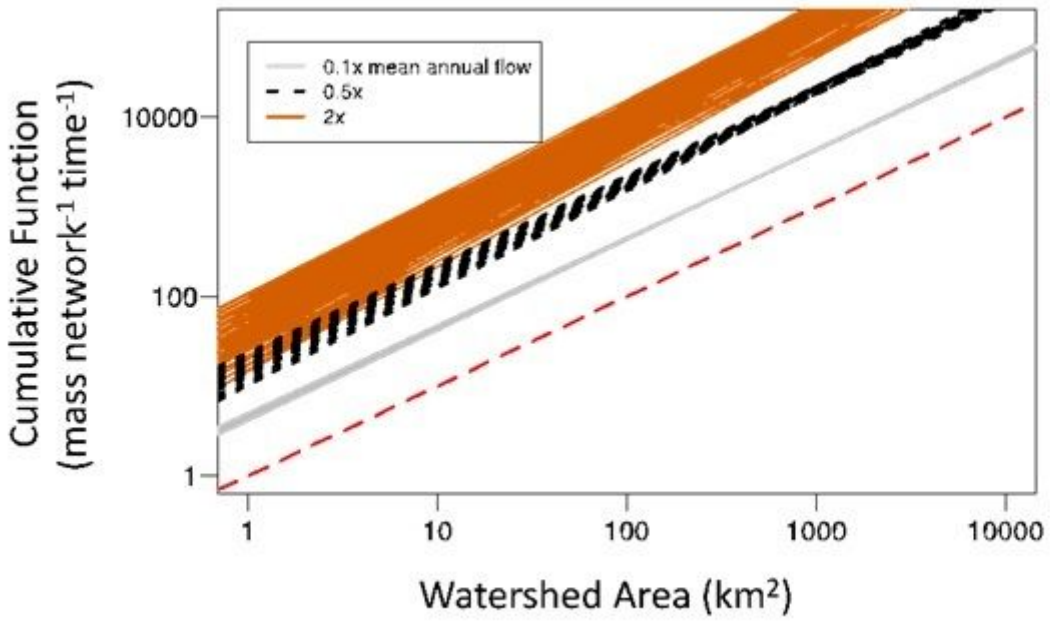

Figure 4

Cumulative biogeochemical function of first-order processes vs. watershed area at different flows. Colors represent flow conditions as a proportion of mean annual flow: 0.1x mean annual flow (grey), 0.5x (black dashed), and 2x (orange). Red dashed line indicates linear scaling. Model results reflect a rectangular river network with average process rate in a 1 km2 headwater watershed = 500 m yr-1 (b in Equation 2). Lines depict potential variation in channel hydraulics and first-order biogeochemical scenarios in Supplementary Table1 (each flow level contains n = 87 scenarios, varying e, f, g, and m.local for first order) .

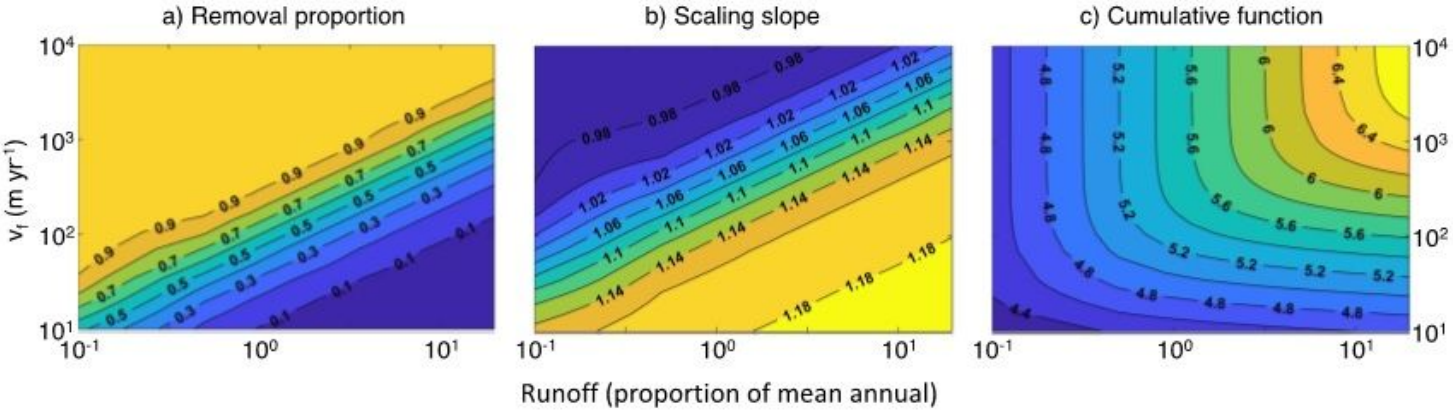

Figure 5

Model scenarios showing the impact of uptake velocity and runoff (as a proportion of mean annual runoff) on A) mean network scale removal (proportion of inputs from land removed by the entire river

network), B) mean scaling slope, d, and C) cumulative aquatic function (kg yr-1 in the modeled river network). Each vf and runoff combination is based on the mean of 27 hydraulic scenarios for a rectangular network as described in Supplementary Table1. Contour intervals indicate the value for each isobar boundary.

Supplementary Files

This is a list of supplementary files associated with this preprint. Click to download.

- MSMetScalingRiverNetworksNatGeoSupplementalV3.docx